Slip flow heat transfer in micro-tubes with viscous dissipation

Nizar Loussif[a,b], Jamel Orfi[c,*]

[a]École Nationale d'Ingénieur de Monastir, Université de Monastir, Monastir, Tunisie
[b]Unité de Recherche Matériaux, Énergie et Énergies Renouvelables, Université de Gafsa, Gafsa, Tunisie
[c]Department of Mechanical Engineering, King Saud University, P.O. Box 800, 11421 Riyadh, KSA
Fax: +966 1 467 6652; email: orfij@ksu.edu.sa

ABSTRACT

A numerical study for a steady-state, two-dimensional, laminar convective heat transfer of a rarefied gas in a micro-tube is conducted using first-order slip velocity and temperature jump boundary conditions and taking into account the viscous dissipation and the axial conduction. The numerical model based on the finite volume method was validated using the available data for fully developed slip flow and developing continuum flow. The study reveals significant impact of slip velocity and temperature jump conditions and viscous dissipation on the velocity and temperature profiles at different sections of the micro-tube. The friction coefficient and the Nusselt number are substantially affected by rarefaction and viscous dissipation. The influence of the viscous dissipation depends on whether the fluid is heated or cooled. For the heating case, the Nusselt number distribution exhibits a special behavior characterized by the existence of a singular point where Nusselt number goes to the infinity. The thermal field development continues after the location of this singular point until reaching the fully developed regime. Furthermore, including viscous dissipation for continuum flow results in a significant increase in the Nusselt number regardless the value of the Brinkman number. Applying the temperature jump boundary condition reduces drastically the heat transfer rates along the micro-tube. The axial conduction improves the heat transfer process in the entrance region of the tube for low Peclet numbers and with no temperature jump condition.

Keywords: Micro-tubes; Slip flow; Jump temperature; Viscous dissipation; Heat conduction

1. Introduction

Flow field and heat transfer at micro-scale have attracted an extensive research interest in recent years due to the rapid development of micro-electro-mechanical systems (MEMS), biomedical applications, innovative cooling techniques for integrated circuits, and separation processes. An understanding of fluid flow with heat transfer in these micro-devices is imperative before the design and fabrication of efficient micro-pumps and micro-actuators.

Micro-channels and micro-tubes are the basic structure in the above systems and devices. Therefore, enormous research work has been conducted on nano- and micro-ducts using different methods, mainly theoretical ones [1–5].

Modeling the fluid flow with heat transfer for such micro-devices is different from that of the

*Corresponding author.

macro-scale systems. For instance, for gas flow, rarefaction effects at the wall must be taken into consideration when the characteristic length is on the order of 100 μm, under normal conditions of temperature and pressure [1]. The ratio of the mean free path to characteristic length known as Knudsen number, Kn = λ/L, defines the region where the continuum assumption is valid and where it becomes no longer valid for the case of gases. For example, when the Knudsen number (Kn) varies between 0.001 and 0.1, the no-slip boundary condition is violated at solid interfaces. The slip at the wall has to be correctly modeled before realistic theoretical and numerical results can be obtained [2].

Therefore, different flow regimes are classified as follows [1,3,6,7]:

(1) For small values of Kn, the continuum model can be used.
(2) For values of Kn varying between 0.001 and 0.1, the flow is in the slip regime. Navier–Stokes equations with slip boundary conditions should be applied.
(3) For $0.1 < \text{Kn} \leq 10$, the flow is in the transition regime.
(4) For Kn higher than 10, the flow is in the free molecular regime.

Several studies mainly analytical and numerical ones investigated the effect of rarefaction and temperature jump condition on the hydrodynamic and thermal fields as well as on the heat transfer rates. The majority of these studies have solved the energy equation when the hydrodynamic flow is considered fully developed for both cases of constant wall temperature and constant wall heat flux [3,7,8].

Larrodé et al. [6] proposed an analytical solution for the developing temperature profiles in an isothermal circular tube. A fully developed slip velocity profile and a temperature jump boundary condition were used. Cetin et al. [7] investigated the effects of axial conduction, rarefaction, and viscous dissipation on the development of the thermal field in micro-tubes. Yu and Ameel [8,9] studied analytically the laminar slip flow forced convection in rectangular micro-channels assuming that the hydrodynamic field is fully developed. Developing and fully developed flow Nusselt numbers were obtained.

Barron et al. [10] extended analytically the original Graetz problem of thermally developing heat transfer in laminar flow through a circular tube to slip flow. Relationships for Knudsen numbers ranging from 0 to 0.12 were developed to describe the effect of slip flow on heat transfer coefficient.

Zhang et al. [5] reported that the rarefaction, viscous heating, surface roughness, and compressibility have significant effects on the flow and heat transfer patterns in the slip flow region. Using the superposition principle, Zhang et al. [5] developed an analytical solution for steady heat transfer in a two-dimensional micro-channel including the effects of the velocity slip and temperature jump at the wall and the viscous heating. The authors assumed the fluid is incompressible and the hydrodynamic field is fully developed. Xiao et al. [11] solved the momentum and the energy equation under slip condition and temperature jump when the flow is assumed to be hydrodynamically fully developed. It was shown that increasing the Knudsen number decreases the maximum velocity inside the tube. Second-order velocity slip boundary condition effects have been also presented. El-Genk and Yang [12] studied numerically the influence of slip and viscous heat dissipation on the friction number of thermally developing laminar water flow in micro-tubes. The effects of the fluid viscosity, the Reynolds number, and the micro-tube diameter on the friction coefficient were presented and discussed. Jeong and Jeong [13] investigated the convective heat transfer in micro-channels for two types of boundary conditions, namely constant wall temperature and constant wall heat flux. The flow was assumed to be hydrodynamically developed but not thermally developed. The study considered the effects of first-order slip velocity, temperature jump, and viscous dissipation. The results show the impact of Knudsen number and Brinkman number, Br, on the temperature profiles and heat transfer rates. Aydin and Avci [14] analysed analytically the effect of velocity slip and temperature jump at the wall of a micropipe. The viscous dissipation was also taken into account. The hydrodynamic and thermal fields were supposed fully developed. Some inconsistencies in their analysis were recently outlined [1]. Later, the same authors [15] extended their study to the conjugate heat transfer in thermally developing flow inside a micro-tube. Chai et al. [16] analyzed compressible gas flows through micro-channels or micro-tubes and developed complete sets of asymptotic solutions using a quasi-isothermal assumption.

The effect of slip flow at a membrane surface of water treatment or desalination systems was studied by few authors. Singh and Laurence focused on the effect of slip velocity at the membrane surface of an ultra-filtration unit on the concentration polarization for tube flow [17] and channel flow systems [18]. The solution of the momentum and the diffusion equations for a uniform permeation rate were obtained analytically using the perturbation method. Recently, Ramon

et al. [19] presented a two-dimensional, boundary layer model describing the heat transfer in the feed channel of a vacuum membrane distillation (VMD) module. The model allows for variations of viscosity with temperature and considers the effect of slip velocity over the liquid–gas interface.

Only few studies have focused on the effects of rarefaction on the simultaneous development of the hydrodynamic and thermal fields in micro-channels or tubes. The very recent work of Kakac et al. [20] is among these studies. The authors analyzed the effect of variable thermal conductivity and viscosity on convective heat transfer in micro-channels and in micro-tubes. In addition, the influence of rarefaction, viscous heating, and axial conduction was investigated numerically using a two-dimensional elliptic model. Two different cases for fluid cooling and fluid heating have been analyzed. Sun and Jaluria [21] analyzed numerically the roles of pressure work and viscous dissipation in pressure-driven nitrogen slip flows in long micro-channels. A two-dimensional model that includes variable properties, first-order velocity slip and temperature jump, and thermal creep was employed. The uniform wall temperature and the uniform wall heat flux boundary conditions were considered. Hadjiconstantinou and Simek [4] noticed that it is necessary to include the effects of axial conduction in the continuum model, since small-scale flows retypically characterized by finite Peclet numbers.

The recent work of Colin [22] is of great importance since it presented a state of the art review on convective heat transfer in micro-channels focusing on rarefaction effects in the slip flow regime. Several analytical and numerical models are compared and commented for various geometries and various types of boundary conditions. Besides, some comments on the first- and second-order formulations are presented. Colin et al. [23] conducted an experimental work on a gaseous flow in rectangular micro-channels to confirm the domain of accuracy of first- and second-order slip model. It was found that the second-order model is valid for Knudsen numbers up to 0.25, whereas the first-order model is no longer accurate for values higher than 0.05.

Liu et al. [24] obtained by separation of variables the solution of the extended Greatz problem of micro-tubes including the heat conduction, viscous dissipation, and thermal entrance effects. The solution of the energy equation is given under constant wall temperature and temperature jump boundary conditions. The effects of velocity slip, temperature jump, Brinkman number, and Peclet number on the local and average heat transfer coefficient are systematically investigated. The heat conduction improves the heat transfer mechanism for low Peclect numbers.

On the other hand, Bahrami et al. [1] investigated some aspects of subsonic-forced convective heat transfer in a micro-tube including rarefaction and viscous dissipation. Two studies have been presented in this work. In the first, the effect of rarefaction and viscous dissipation in the fully developed region is analytically investigated. In the second study, a numerical model for the developing flow is employed to analyze the simultaneous effects of rarefaction, viscous dissipation, and axial conduction. These effects may become important for dilute gas flows depending on the operating conditions [1].

The inspection of the above-reported studies reveals that only very few works focussed on the simultaneous development of convective heat transfer in micro-tubes by taking into account the rarefaction, the viscous dissipation, and axial conduction effects.

In the present work, a numerical study for the steady-state, two-dimensional, simultaneously developing laminar convective heat transfer of a rarefied gas in a micro-tube is conducted using first-order slip velocity and temperature jump conditions. The effects of rarefaction and viscous dissipation on the friction factor and the Nusselt number are presented. Detailed results on the development of the velocity and temperature profiles along the micro-tube as well as on the axial distribution of the heat transfer coefficient for different values of Knudsen and Brinkman numbers are investigated.

2. Analysis and modeling

A simultaneously developing flow in a micro-tube is investigated under slip velocity and temperature jump conditions. The coordinate system and geometry are shown in Fig. 1.

The main assumptions used in this study are: steady state, axis-symmetric, and constant fluid properties flow with negligible gravitational forces.

The governing equations of conservation of mass, momentum, and energy are expressed as [25]:

$$\frac{D\rho}{Dt} + \rho \nabla \cdot \vec{V} = 0 \tag{1}$$

$$\rho \frac{D\vec{V}}{Dt} = -\nabla P + \mu \nabla^2 \vec{V} \tag{2}$$

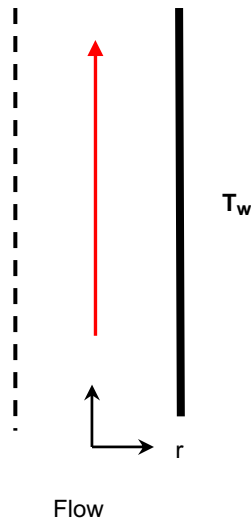$$\rho c_p \frac{DT}{Dt} = k \nabla^2 T + \mu \Phi \tag{3}$$

$$\left(\bar{V}\frac{\partial \bar{V}}{\partial \bar{r}} + \bar{U}\frac{\partial \bar{V}}{\partial \bar{z}}\right) = -\frac{\partial \bar{P}}{\partial \bar{r}} + \frac{1}{\mathrm{Re}}\left[\frac{1}{\bar{r}}\frac{\partial}{\partial \bar{r}}\left(\bar{r}\frac{\partial \bar{V}}{\partial \bar{r}}\right) - \frac{\bar{V}}{\bar{r}^2} + \frac{\partial^2 \bar{V}}{\partial \bar{z}^2}\right]$$

(7)

$$\left(\bar{V}\frac{\partial \bar{U}}{\partial \bar{r}} + \bar{U}\frac{\partial \bar{U}}{\partial \bar{z}}\right) = -\frac{\partial \bar{P}}{\partial \bar{z}} + \frac{1}{\mathrm{Re}}\left[\frac{1}{\bar{r}}\frac{\partial}{\partial \bar{r}}\left(\bar{r}\frac{\partial \bar{U}}{\partial \bar{r}}\right) + \frac{\partial^2 \bar{U}}{\partial \bar{z}^2}\right]$$

(8)

$$\left(\bar{V}\frac{\partial \bar{T}}{\partial \bar{r}} + \bar{U}\frac{\partial \bar{T}}{\partial \bar{z}}\right) = \frac{1}{\mathrm{Re\,Pr}}\left[\frac{1}{\bar{r}}\frac{\partial}{\partial \bar{r}}\left(\bar{r}\frac{\partial \bar{T}}{\partial \bar{r}}\right) + \frac{\partial^2 \bar{T}}{\partial \bar{z}^2}\right]$$
$$+ \frac{\mathrm{Br}}{\mathrm{Re\,Pr}}\left\{2\left[\left(\frac{\partial \bar{V}}{\partial \bar{r}}\right)^2 + \left(\frac{\bar{V}}{\bar{r}}\right)^2 + \left(\frac{\partial \bar{U}}{\partial \bar{z}}\right)^2\right]\right.$$
$$\left. + \left(\frac{\partial \bar{V}}{\partial \bar{z}} + \frac{\partial \bar{U}}{\partial \bar{r}}\right)^2\right\}$$

(9)

Fig. 1. Geometry and coordinate system of flow domain.

In these equations, $\vec{V}$ is the velocity vector (U, V), D/Dt represents the material derivative operator. ρ, μ, c_p, k are the fluid density, dynamic viscosity, specific heat, and thermal conductivity, respectively. Φ represents the viscous dissipation function. For the case of a two-dimensional axisymmetric problem, it is expressed as [25]:

$$\Phi = 2\left[\left(\frac{\partial V}{\partial r}\right)^2 + \left(\frac{V}{r}\right)^2 + \left(\frac{\partial U}{\partial z}\right)^2 + \frac{1}{2}\left(\frac{\partial V}{\partial z} + \frac{\partial U}{\partial r}\right)^2\right.$$
$$\left. - \frac{1}{3}(\nabla \cdot \vec{V})^2\right]$$

(4)

The preceding equations can be written in a non-dimensional form using the following quantities:

$$\bar{r} = \frac{r}{R}, \bar{z} = \frac{z}{R}, \bar{V} = \frac{V}{U_{\mathrm{in}}}, \bar{U} = \frac{U}{U_{\mathrm{in}}}, \bar{P} = \frac{P}{\rho U_{\mathrm{in}}^2}, \bar{T} = \frac{T - T_{\mathrm{w}}}{T_{\mathrm{in}} - T_{\mathrm{w}}}$$

(5)

where R is the radius of the micro-tube, U_{in} and T_{in} are, respectively, the inlet velocity and the inlet temperature of the fluid, T_{w} is the wall temperature.

Upon substitution, the resulting non-dimensional mass, momentum, and energy conservation equations expressed in cylindrical coordinates are:

$$\frac{1}{\bar{r}}\frac{\partial}{\partial \bar{r}}\left(\bar{r}\bar{V}\right) + \frac{\partial}{\partial \bar{z}}\left(\bar{U}\right) = 0$$

(6)

The boundary conditions are:

At the tube inlet $\bar{z} = 0$, uniform axial velocity and uniform temperature are imposed.

$$\bar{U} = 1; \ \bar{V} = 0; \ \bar{T} = 1$$

(10)

At $\bar{r} = 0$, the symmetry condition is expressed as:

$$\bar{V} = 0; \ \frac{\partial \bar{U}}{\partial \bar{r}} = 0; \ \frac{\partial \bar{T}}{\partial \bar{r}} = 0$$

(11)

At $\bar{r} = 1$, the normal velocity is zero, since the wall is impermeable while the usual no-slip condition does not apply. A temperature jump at the wall surface is considered.

$$\bar{V} = 0$$

(12)

$$\bar{U} = -2\beta_{\mathrm{v}}\mathrm{Kn}\left.\frac{\partial \bar{U}}{\partial \bar{r}}\right|_{\bar{r}=1}$$

(13)

$$\bar{T} = -2\beta_t\mathrm{Kn}\left.\frac{\partial \bar{T}}{\partial \bar{r}}\right|_{\bar{r}=1}$$

(14)

where

$$\beta_{\mathrm{v}} = \frac{(2 - f_{\mathrm{v}})}{f_{\mathrm{v}}}$$

(15a)

$$\beta_t = \frac{2 - f_t}{f_t}\frac{2\gamma}{1 + \gamma}\frac{1}{\mathrm{Pr}}$$

(15b)

At the tube outlet $z = L$, the first derivative of the velocity components and temperature is taken to be zero.

$$\frac{\partial \bar{U}}{\partial \bar{z}} = 0; \quad \frac{\partial \bar{V}}{\partial \bar{z}} = 0; \quad \frac{\partial \bar{T}}{\partial \bar{z}} = 0 \qquad (16)$$

Eqs. (13) and (14) give the first-order slip velocity and temperature jump conditions as adopted by Larrode et al. [6] and Bahrami et al. [1].

The above coefficients f_v and f_t are known as the tangential momentum accommodation coefficient and thermal accommodation coefficient, respectively. These parameters describe the gas–surface interaction and are functions of the composition, temperature, and pressure of the gas, the gas velocity over the surface, the solid surface temperature, and roughness. Their values range from near 0 to 1. For most engineering applications, these coefficients are taken to be close to unity [8,20].

The ratio of β_t to β_v can be introduced as β. Its values can range from 0 to more than 100 [8]. In this work, β_v will be considered as equal to unity. A typical value of β for many engineering applications is 1.667. This value corresponds to $f_v = 1$, $f_t = 1$, $\gamma = 1.4$ and $Pr = 0.7$.

It is of interest to mention that the above set of equations with the boundary conditions are governed by five non-dimensional parameters: Reynolds number, Re, Prandtl number, Pr, Brinkman number, Br, Knudsen number, Kn, and the ratio of the accommodation coefficients, β.

For a fully developed velocity profile, the analytical solutions for the axial velocity and the friction coefficient in non-dimensional form are:

$$\bar{U} = \frac{2(1 - \bar{r}^2) + 8\beta_v Kn}{1 + 8\beta_v Kn} \qquad (17)$$

$$fRe = \frac{16}{1 + 8\beta_v Kn} \qquad (18)$$

3. Numerical model and validation

The above set of two-dimensional fully elliptic governing Eqs. (6)–(9) with the appropriate boundary conditions (10–16) is solved numerically using the control volume method and the **simpler** algorithm [26].

Table 1 shows that the computed centerline velocity and Nusselt number values are almost the same for the three considered grids. The number of nodes

retained for the simulations was chosen to be 1000 × 80, respectively, in the axial and radial directions.

The proposed model was validated with the available data from literature. As shown in Table 2, the centerline velocity and friction coefficient for fully developed flow are in good agreement with the exact solutions given in Eqs. (17) and (18). In Tables 3 and 4, the computed fully developed Nusselt number is compared with the results of Cetin et al. [3] for the cases of slip flows with and without viscous dissipation.

Furthermore, the axial evolutions of the developing Nusselt number and friction factor corresponding to the continuum model (Kn = 0) were computed and compared with the results of Jensen [27] and Hornbeck [28]. Fig. 2 shows an excellent agreement between our results and the previous results.

In all of these validation tests, the agreements are found to be fairly good. Therefore, the numerical model is reliable and can be used for the analysis of confined forced convection in micro-tubes.

Table 1
Grid dependence study

	Fully developed centerline velocity		Fully developed Nusselt number, $\beta = 0.5$	
	(Kn = 0)	(Kn = 0.12)	(Br = 0, Kn = 0)	(Br ≠ 0, Kn = 0.12)
1,000 × 80	1.9991	1.5100	3.6573	6.4371
800 × 60	1.9988	1.5096	3.6580	6.4379
600 × 40	1.9987	1.509	3.6583	6.4383

Table 2
Fully developed centerline velocity and friction coefficient

Kn	Fully developed centerline velocity		Fully developed fRe	
	Analytical solution	This study	Analytical solution	This study
0	2.0000	1.9991	16.0000	16.0011
0.02	1.8620	1.8616	13.7931	13.7944
0.04	1.7575	1.7571	12.1212	12.1227
0.06	1.6756	1.6753	10.8108	10.8122
0.08	1.6097	1.6094	09.7560	09.7573
0.1	1.5555	1.5553	08.8888	08.8899
0.12	1.5102	1.5100	08.1632	08.1642

Table 3
Fully developed Nu numbers (Br = 0)

Kn	Nu, $\beta = 0$		Nu, $\beta = 0.5$		Nu, $\beta = 1.667$	
	[3]	This study	[3]	This study	[3]	This study
0	3.656	3.6573	3.656	3.6573	3.656	3.6573
0.02	3.855	3.8558	3.739	3.7398	3.488	3.4884
0.04	4.020	4.0207	3.778	3.7784	3.292	3.2919
0.06	4.160	4.1599	3.785	3.7848	3.087	3.0873
0.08	4.279	4.2787	3.767	3.7671	2.887	2.8867
0.10	4.382	4.3813	3.732	3.7316	2.697	2.6968
0.12	–	4.4710	–	3.6832	–	2.5210

Table 4
Fully Developed Nu numbers (Br $\neq$ 0)

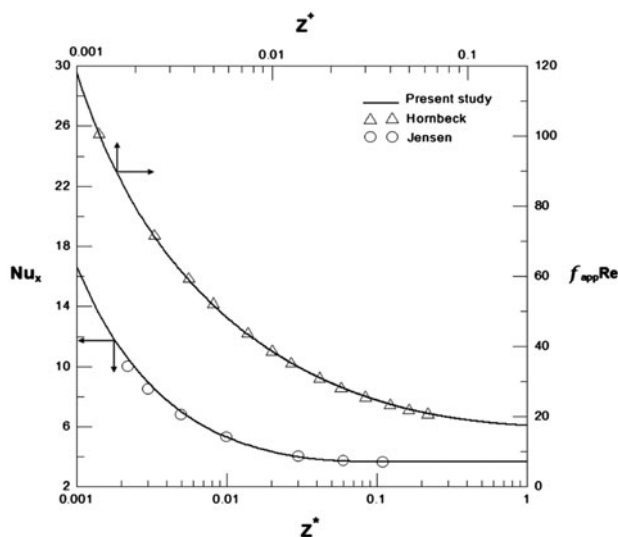| Kn	Nu, $\beta = 0$		Nu, $\beta = 0.5$		Nu, $\beta = 1.667$	
	[3]	This study	[3]	This study	[3]	This study
0	9.598	9.5971	9.598	9.5971	9.598	9.5971
0.02	9.871	9.8692	8.984	8.9810	7.427	7.4248
0.04	10.088	10.0839	8.394	8.3912	6.031	6.0274
0.06	10.264	10.2629	7.848	7.8469	5.065	5.0609
0.08	10.441	10.4400	7.350	7.3459	4.359	4.3555
0.10	10.535	10.5312	6.900	6.8871	3.822	3.8197
0.12	–	10.6614	–	6.4371	–	3.3841

Fig. 2. Comparison of the computed results to the results of Jenson [27] and Hornbeck [28].

4. Results and discussion

In order to study the effects of rarefaction on the developing hydrodynamic and thermal fields of a laminar forced flow in a micro-tube with viscous dissipation, several simulations were performed first for fixed Peclet number of 24.5 (Re = 35 and Pr = 0.7). The effect of axial conduction is also considered for a wide range of Peclet numbers. The length to the radius ratio of the micro-tube is equal to 100.

4.1. Hydrodynamic field

Fig. 3 presents the distribution of the axial velocity profiles for three different sections (z/R = 3, 10, 100) and different degrees of rarefaction. One can see that when the slip flow condition is applied, the fluid particles adjacent to the solid surface of the tube wall no longer attain the velocity of the solid surface. In the core region of the tube, the fluid decelerates and its maximum velocity occurring at the centerline of the tube decreases significantly reaching a value of 1.51 for Kn = 0.12. This phenomenon is described clearly in Fig. 4 where the evolution of the centerline and wall velocities across the micro-tube for different rarefaction degrees is presented. One can see that increasing the rarefaction induces a decrease of the centerline velocity, while the streamwise fluid velocity at the wall is no longer zero and can reach 0.5 for high Kn numbers. This behavior for the fully developed region can be obtained by the exact velocity profile given by Eq. (17).

Fig. 5 presents the axial distribution of the friction coefficient for different values of Kn. It is of interest to recall that the friction coefficient is expressed in terms of the axial velocity gradient at the tube wall. For the no-slip case, the apparent friction coefficient is higher than that of the slip flow case. It reaches the usual value of 16 when the flow becomes fully developed. When a tangential slip-velocity boundary condition is taken into consideration, a decrease of the apparent friction coefficient occurs along the tube. This decrease is very significant at the tube entrance and leads to almost a uniform distribution of this coefficient along the micro-tube length. This phenomenon is a direct consequence of the flattening of the velocity profiles observed previously.

4.2 Thermal field

The Brinkman number, Br, is introduced to account for the influence of viscous dissipation such as heating or cooling of the viscous fluid due to
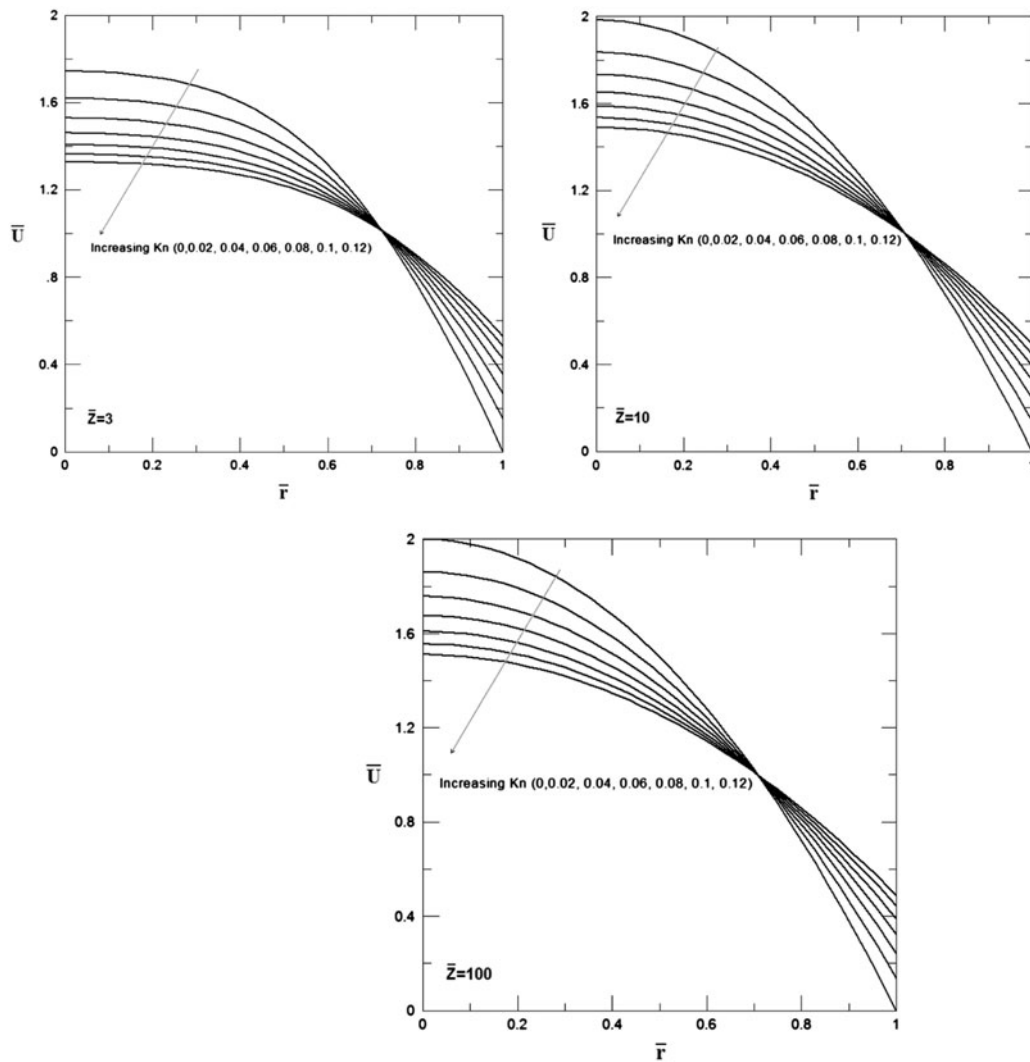
Fig. 3. Evolution of the axial velocity profiles for different degrees of rarefaction.

internal friction. Brinkman number approaches zero when the viscous dissipation is negligible. It takes negative values when the fluid is heated at the wall (wall temperature is higher than the inlet fluid temperature), while for the cooling case, Br is positive.

Fig. 6 illustrates the radial distribution of the temperature profile at the micro-tube exit for different values of Br numbers. One can observe that for the basic case of no-slip flow (Kn = 0) and negligible viscous dissipation (Br = 0), the non-dimensional temperature is zero at the surface wall as expected, since no jump occurs and is also zero in the core region of the tube indicating that the fluid temperature has already reached the wall temperature.

For the no-slip flow case, increasing (decreasing) Br numbers will increase (decrease) the non-dimen-

sional temperature particularly near the tube center. For the slip conditions, the situation depends also on the Kn and β parameters referring to the slip velocity and temperature jump at the wall. One can see that applying the temperature jump condition (Kn = 0.12, β = 1.667) induces an increase in the non-dimensional temperature not only in the vicinity of the tube wall but also in the tube core region. It seems that there is a kind of competition between applying the temperature jump and the viscous dissipation for the heating case; they have opposing effects on the values of temperature profiles.

The effect of slip flow and viscous dissipation on the axial distribution of the fluid wall temperature is depicted in Fig. 7. As observed in Fig. 6, for Kn = 0 (continuum) or β = 0 (no temperature jump), the
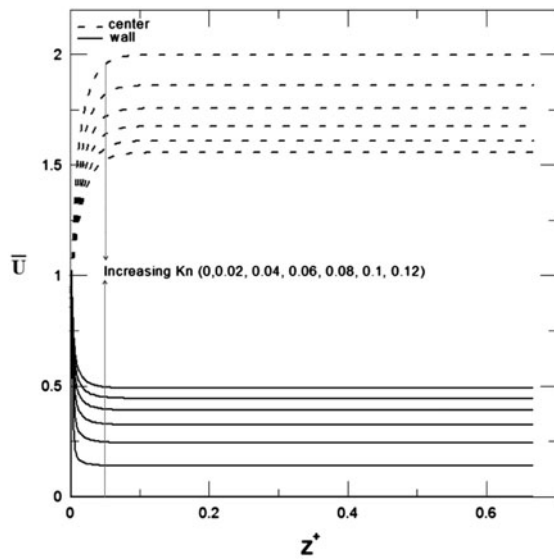
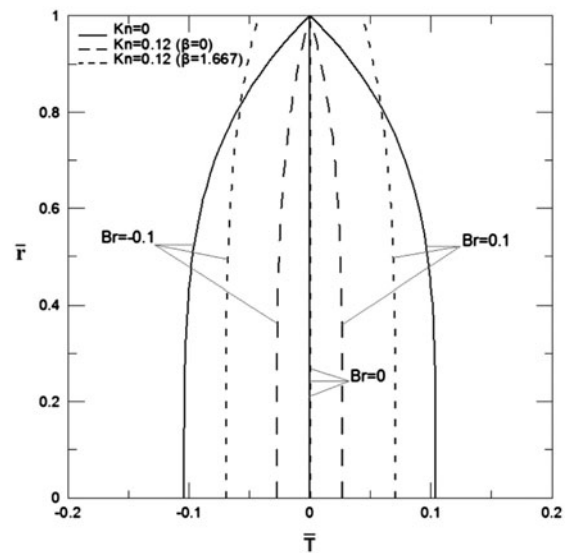Fig. 4. Evolution of the centerline and wall velocities as a function of z^+ for different values of Kn.

Fig. 6. Temperature profile at the outlet of the tube for different slip velocity (continuum and Kn = 0.12) and temperature jump degrees (0 and 1.667) and parameterized by Br numbers.
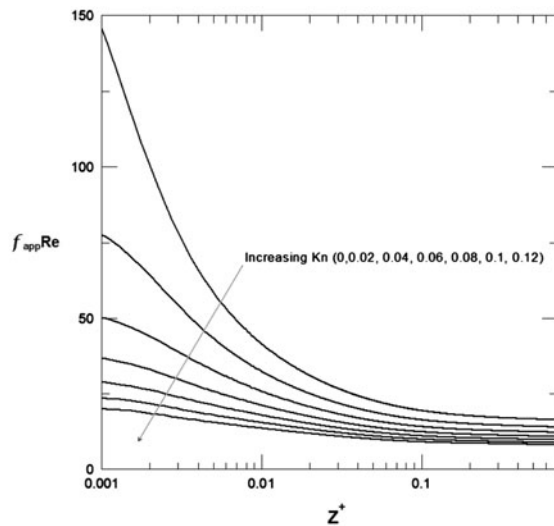

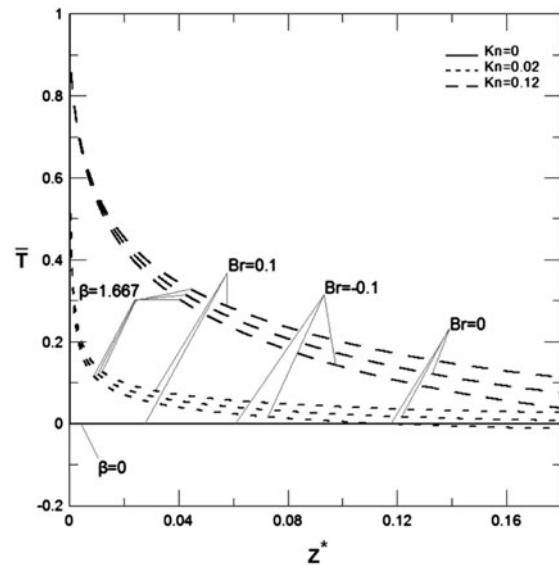Fig. 5. Axial variation of the apparent friction coefficient for different rarefaction values.

Fig. 7. Fluid temperature at the tube wall.

normalized temperature of the fluid at the wall remains constant and equal to zero. For $\beta \neq 0$, the non-dimensional fluid temperature at the wall surface decreases with the axial coordinate and tends towards zero near the tube exit. It increases for a fixed axial position when Kn increases from 0.02 to 0.12.

Fig. 8 depicts the distribution of the fully developed Nusselt number as function of Kn, β, and Br. For the case of no temperature jump ($\beta = 0$), the heat transfer rate at the wall increases linearly with the Knudsen number for both cases, with and without

viscous dissipation. Increasing β from 0.5 to 10 reduces the Nusselt number values for a fixed Knudsen number. This reduction is very important for the case with viscous dissipation. It is also of interest to focus on the particular value of $\beta = 1.667$ where the fully developed Nusselt number tends for high Kn to approximately 2 and 4 for the case without and with viscous dissipation, respectively. These values remain close to the well-known value of 3.66 corresponding
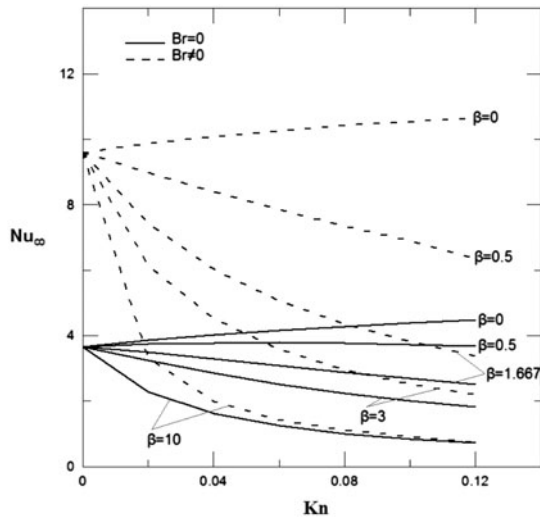
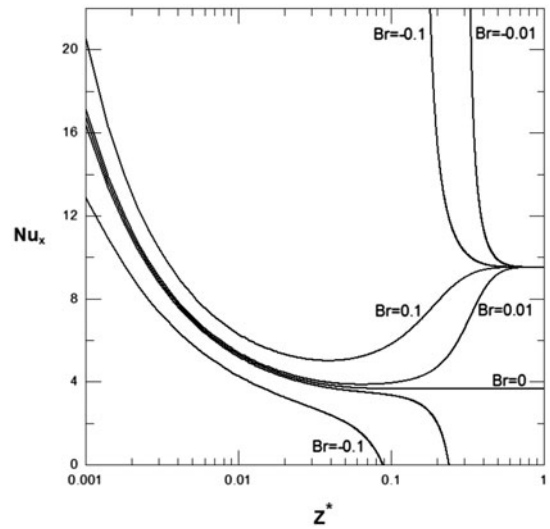Fig. 8. Fully developed Nusselt number as function of Kn, β, and Br.

Fig. 9. Axial variation of the local Nusselt for different values of *Br* (Kn = 0).

to the standard case of fully developed flow without slip and with negligible viscous dissipation.

Fig. 9 presents the local Nusselt number distribution along the micro-tube for the continuum flow with viscous dissipation. Fully developed Nusselt number reaches two different values namely 3.66 and 9.59 for the cases of Br = 0 and Br ≠ 0, respectively. Therefore, including viscous dissipation results in a significant increase in the Nusselt number regardless the value of the Brinkman number. A negative Br for this constant wall temperature boundary condition refers to the fluid being heated as it flows along the tube (wall temperature is higher than entrance fluid temperature), while the viscous dissipation tends to reinforce the external heating effect. If we neglect the viscous dissipation, the bulk temperature tends to the wall temperature without reaching it. However, when the viscous dissipation is taken into account, the bulk temperature increases at a higher rate due to the additional effect of the heating by the friction among fluid molecules. Therefore, the bulk temperature can reach the wall temperature along the tube length. The particular location where the bulk temperature is equal to the wall temperature corresponds to a singular point where the local Nusselt number goes to the infinity. This particular location in the tube length depends on the value of Br; it moves downstream when the absolute value of Br decreases. For fixed values of Br and before the particular location of the singular point, the wall heat flux is positive: the wall heats the fluid. After the singular point location, the fluid heats the wall and heat flux is negative.

It important to note that similar observations were also reported by several authors such us Liu et al. [24] for the thermally developing field in isothermal circular micro-channels. For the cooling case (positive Br number), the local Nusselt number decreases in the entrance region of the tube, increases at an intermediate axial position, and approaches the constant value of 9.59 near the tube exit. Similar behavior has been observed by Kakac et al. [20].
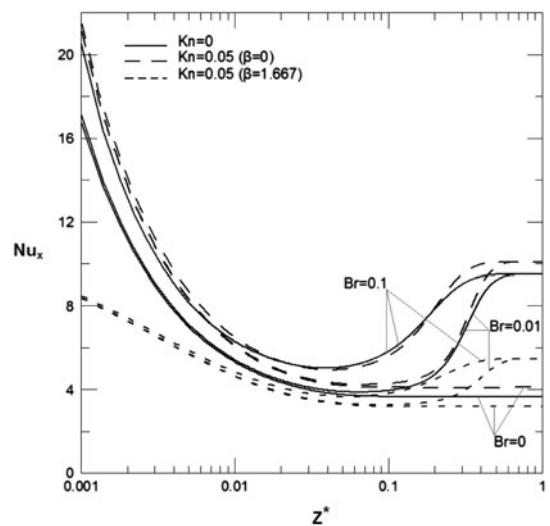

Fig. 10. Variation of local Nu as a function of non-dimensional axial coordinate for different β, Kn, and positive Br numbers.
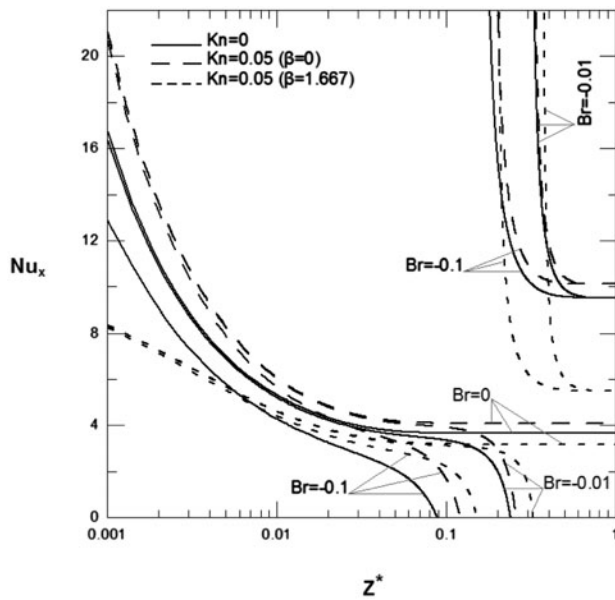
Fig. 11. Variation of local Nusselt number for different β, Kn and negative values of Br.

Fig. 10 shows the evolution of local Nusselt number along the micro-tube for positive Br when Kn = 0.05. Two values of β (β = 0, 1.667) are considered. When β = 0 (no temperature jump), the behavior of the local heat transfer coefficient is similar to the case of continuum model (Kn = 0). The Nusselt number decreases in the entrance region of the micro-tube and then increases in the fully developed region, except when Br = 0. For this latter case (Br = 0), we obtain the known behavior for which the fully

developed Nussselt number tends to the asymptotic value of 3.66. When increasing the value of β to 1.667 (temperature jump for air flow), the heat transfer rates are reduced drastically not only in the fully developed region but also in the tube entrance. The effect of viscous dissipation is noticeable only in the vicinity of the tube exit region.

It is also important to note that when considering the viscous dissipation effects, the type of boundary condition at the tube wall defines the value of asymptotic Nusselt number.

The axial distribution of the local Nusselt number for negative values of Brinkman number is presented in Fig. 11. In this case, the fluid is being heated along the micro-tube. As observed in Fig. 9, the Nusselt number exhibits a particular behavior when the bulk temperature reaches the wall temperature. The thermal field development continues after the location of the singular point until reaching the fully developed regime. Similar to positive Br cases, applying the temperature jump condition reduces the heat transfer rates along the whole tube length. Besides, for fixed values of Kn and β, the fully developed Nusselt number converges to the same value as it is the case for positive Br.

Peclet number is a measure of the relative importance of axial convection to axial conduction. If this number is small, axial conduction will be of importance. Figs. 12 and 13 depict the effect of axial conduction for Kn = 0.05. Negative and positive values of Br are considered in these figures. It is found that this effect is limited to the entrance region of micro-tube where the thermal and hydrodynamic fields are under
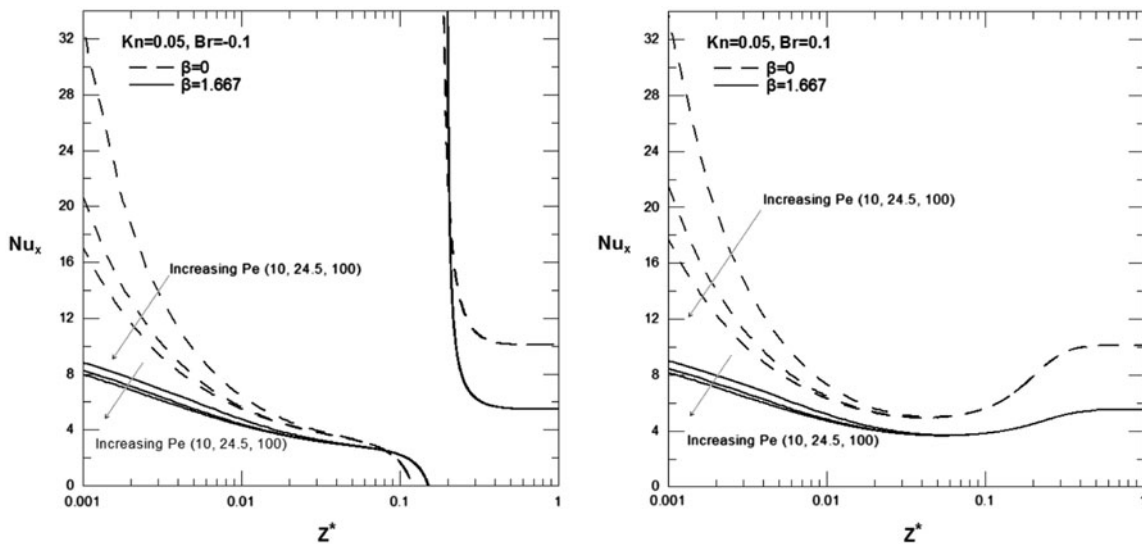

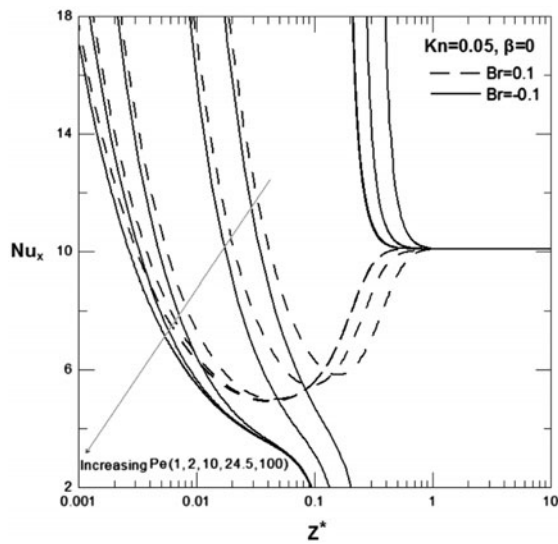Fig. 12. Effect of Peclet number on the axial variation of Nusselt number for Br = −0.1 and Br = 0.1.

Fig. 13. Effect of Peclet number on the axial variation of Nusselt number for Br = −0.1 and Br = 0.1 and for β = 0.

development. However, in the fully developed region, the value of Peclet has no effect on Nusselt number. On the other side, the influence of Pe is seen to be more significant for the case of β = 0, while for β = 1.667, this influence is weak even in the region close to micro-tube inlet. Fig. 13 includes results for very low values of Peclet (Pe = 1 and 2). One can see that the effect of axial diffusion is still present even far from the tube entrance.

5. Conclusion

Simultaneously developing laminar flow in an isothermal micro-tube was studied numerically using first-order slip velocity and temperature jump boundary conditions applied to the continuum mass, momentum, and energy equations. The axial conduction and viscous dissipation were taken into account in the energy equation. The obtained results were presented in terms of development of velocity and temperature profiles and axial distributions of the heat transfer coefficient and the friction factor for different Knudsen number, coefficient β, and Brinkman number. The main results of this study can be summarized as follows:

(1) The hydrodynamic flow was found to be dependent on the degree of rarefaction represented by the Knudsen number, Kn. Increasing Kn reduces the axial velocity of the tube center, increases the streamwise fluid velocity at the wall and induces a flattening of the velocity profiles.

(2) The behavior of the heat transfer mechanism depends on whether the temperature jump boundary condition is considered or not. It was observed that a significant decrease of the values of Nusselt number happens in particular for high values of β.

(3) The influence of the viscous dissipation depends if the fluid is heated (negative Br) or it is cooled (positive Br). For the heating case, the Nusselt number distribution exhibits a special behavior characterized by the existence of a singular point where Nusselt number goes to the infinity. The thermal field development continues after the location of this singular point until reaching the fully developed regime.

(4) Axial conduction improves the heat transfer mechanism in the entrance region of the micro-tube for low Peclet numbers and when β = 0 (no temperature jump).

Symbols

Br	—	Brinkman number, $\frac{U_{in}^2 \mu}{(T_{in}-T_w)k}$
c_p	—	specific heat at constant pressure
D	—	tube diameter
f_t	—	thermal accommodation coefficient
f_v	—	tangential momentum accommodation
f_{app}	—	apparent friction coefficient, $\frac{\Delta P r_h}{\rho U_{in}^2 Z/2}$
h	—	convective heat transfer coefficient
k	—	thermal conductivity
Kn	—	Knudsen number, λ/D
L	—	micro-tube length
Nu_x	—	local Nusselt number, $h_x D/k$
P	—	pressure
Pr	—	Prandtl number, $\mu c_p/k$
r	—	radial coordinate
r_h	—	hydraulic radius
$\bar{r}$	—	non-dimensional radial coordinate, r/R
R	—	micro-tube radius
Re	—	Reynolds number, $U_{in}\, \rho R/\mu$
T	—	temperature
$\bar{T}$	—	non-dimensional temperature
U	—	velocity component in the z-direction
$\bar{U}$	—	non-dimensional velocity component in the z-direction
V	—	velocity component in the r-direction

$\bar{V}$	—	non-dimensional velocity component in the r-direction
z	—	axial coordinate
$\bar{z}$	—	non-dimensional axial coordinate, z/R
z^*	—	non-dimensional axial coordinate, $z/2DRePr$
z^+	—	non-dimensional axial coordinate, $z/2DRe$

Greek

β_v	—	$(2-f_v)/f_v$
β	—	$\frac{2-f_t}{f_t}\frac{2\gamma}{1+\gamma}\frac{1}{\mathrm{Pr}}$
γ	—	ratio of specific heats
λ	—	gas mean free path
μ	—	dynamic viscosity
ρ	—	fluid density

Subscripts

in	—	inlet
m	—	mean
w	—	wall

References

[1] H. Bahrami, T.L. Bergman, A. Faghri, Forced convective heat transfer in a microtube including rarefaction, viscous dissipation and axial conduction effects, Int. J. Heat Mass Transfer 55 (2012) 6665–6675.

[2] A. Agrawal, L. Djenidi, R.A. Antonia, Simulation of gas flow in microchannels with a sudden expansion or contraction, J. Fluid Mechanics 530 (2005) 135–144.

[3] B. Cetin, H. Yuncu, S. Kakac, Gaseous flow in microconduits with viscous dissipation, Int. J. Trans. Phenomena 8 (2007) 297–315.

[4] N. Hadjiconstntinou, O. Simek, Constant wall temperature Nusselt number in micro and nano channels, J. Heat Transfer 124 (2002) 356–364.

[5] T. Zhang, L. Jia, L. Yang, Y. Jaluria, Effect of viscous heating on heat transfer performance in microchannel slip flow regime, Int. J. Heat Mass Transfer 53 (1010) 4927–4934.

[6] F.E. Larrode, C. Housiadas, Y. Drossinos, Slip-flow heat transfer in circular tubes, Int. J. Heat Mass Transfer 43 (2000) 2669–2680.

[7] B. Cetin, A. Yazicioglu, S. Kakac, Fluid flow in microtubes with axial conduction including rarefaction and viscous dissipation, Int. Com. Heat Mass Transfer 35 (2008) 535–544.

[8] S. Yu, T.A. Ameel, Slip flow heat in rectangular microchannels, Int. J. Heat Mass Transfer 44 (2001) 4225–4234.

[9] S. Yu, T.A. Ameel, Slip-flow convection in isoflux rectangular microchannels, J. Heat Transfer 124 (2002) 346–355.

[10] R.F. Barron, X. Wang, R.O. Warringtonand, T.A. Ameel, Evaluation of the eigenvalues for the Graetz problem in slip-flow, Int. Com. Heat Mass Transfer 23 (1996) 563–574.

[11] N. Xiao, J. Elsnab, T.A. Ameel, Microtube gas flows with second-order slip flow and temperature jump boundary conditions, Int. J. Thermal Sci. 48 (2009) 243–251.

[12] M.S. El-Genk, I.H. Yang, A numerical analysis of laminar flow in micro-tubes with a slip boundary, Energy Convers. Manage. 50 (2009) 1481–1490.

[13] H.E. Jeong, J.T. Jeong, Extended Graetz problem including streamwise conduction and viscous dissipation in microchannel, Int. J. Heat Mass Transfer 49 (2006) 2151–2157.

[14] O. Aydin, M. Avci, Heat and fluid flow characteristics of gases in micropipes, Int. J. Heat Mass Transfer 49 (2006) 1723–1730.

[15] M. Avci, O. Aydin, E. Arici, Conjugate Heat Transfer with viscous dissipation in a microtube, Int. J. Heat Mass Transfer 55 (2012) 5302–5308.

[16] C. Cai, Q. Sun, I.D. Boyd, Gas flows in microchannels and microtubes, J. Fluid Mech. 589 (2007) 305–314.

[17] R. Singh, R.L. Laurence, Influence of slip velocity at a membrane surface on ultrafiltration performance—I. Channel flow system, Int. J. Heat Mass Transfer 22 (1979) 721–729.

[18] R. Singh, R.L. Laurence, Influence of slip velocity at a membrane surface on ultrafiltration performance—II. Tube flow system, Int. J. Heat Mass Transfer 22 (1979) 731–737.

[19] G. Ramon, Y. Agnon, C. Dosretz, Heat transfer in vacuum membrane distillation: Effect of velocity slip, J. Membr. Sci. 331 (2009) 117–125.

[20] S. Kakac, A.G. Yazicloglu, A.C. Gozukara, Effect of variable thermal conductivity and viscosity on single phase convective heat transfer in slip flow, Heat Mass Transfer 47 (2011) 879–891.

[21] Z. Sun, Y. Jaluria, Convective heat transfer in pressure-driven nitrogen slip flows in long microchannels: The effects of pressure work and viscous dissipation, Int. J. Heat Mass Transfer 55 (2012) 3488–3497.

[22] S. Colin, Gas microflows in the slip flow regime: A critical review on convective heat transfer, ASME J. Heat Transfer 134 (20908) (2012) 1–13.

[23] S. Colin, P. Lalonde, R Caen, Validation of a second-order slip flow model in rectangular microchannels, Heat Transfer Eng. 25 (2004) 23–30.

[24] H.L. Liu, X.D. Shao, J.Y. Jia, Effects of axial heat conduction and viscous dissipation on heat transfer in circular micro-channels, Int. J. Thermal Sci. 66 (2013) 34–41.

[25] A. Bejan, Convective Heat Transfer, 3rd ed., John Wiley, New Jersey, NJ, 2004, p. 694.

[26] H.K. Versteeg, W. Malalasekera, An Introduction to Computational Fluid Dynamics: The Finite Volume Method, 2nd ed., Pearson and Prentice Hall, Essex, 2007.

[27] M.K. Jensen, Simultaneously developing laminar flow in an isothermal circular tube, Int. Comm. Heat Mass Transfer 16 (1989) 811–820.

[28] R.W. Hornbeck, Laminar flow in the entrance region of a pipe, Appl. Sci. Res., Sect. A 13 (1964) 224–232.